Atmospheric Environment 180 (2018) 11–22

Contents lists available at ScienceDirect

Atmospheric Environment

journal homepage: www.elsevier.com/locate/atmosenv

Review article

A new approach for modeling dry deposition velocity of particles

M. Giardina*, P. Buffa

Department of Energy, Information Engineering and Mathematical Models (DEIM), University of Palermo, Viale delle Scienze, Edificio 6, 90128, Palermo, Italy

ARTICLE INFO

Keywords:
Particle flux
Dry deposition velocity
Parametrization
Removal processes
Radioactive pollutants

ABSTRACT

The dry deposition process is recognized as an important pathway among the various removal processes of pollutants in the atmosphere. In this field, there are several models reported in the literature useful to predict the dry deposition velocity of particles of different diameters but many of them are not capable of representing dry deposition phenomena for several categories of pollutants and deposition surfaces. Moreover, their applications is valid for specific conditions and if the data in that application meet all of the assumptions required of the data used to define the model. In this paper a new dry deposition velocity model based on an electrical analogy schema is proposed to overcome the above issues. The dry deposition velocity is evaluated by assuming that the resistances that affect the particle flux in the Quasi-Laminar Sub-layers can be combined to take into account local features of the mutual influence of inertial impact processes and the turbulent one. Comparisons with the experimental data from literature indicate that the proposed model allows to capture with good agreement the main dry deposition phenomena for the examined environmental conditions and deposition surfaces to be determined. The proposed approach could be easily implemented within atmospheric dispersion modeling codes and efficiently addressing different deposition surfaces for several particle pollution.

1. Introduction

The dry deposition process, which controls the transfer of pollutants from the atmosphere to the surface, is of interest to several disciplines, such as industrial emissions, natural dust, trace metals, chemicals, etc. In the nuclear field, if event of a severe accident and the release of radionuclides in the atmosphere occurs, certain key challenges arise, such as characterizing the specific types of release as well as studying the dispersion and deposition phenomena useful for defining effective mitigation measures and actions to protect the population.

As highlighted in ATMES (Atmospheric Transport Model Evaluation Study) report (Klug et al., 1992), the greatest number of uncertainties in numerical evaluations of pollutant transport and dispersion in air are introduced by the parameterizations both of the source term and deposition velocities.

There is no single accepted theoretical description of the dry deposition phenomena due to the complexity of the fluid-dynamic processes that influence the deposition flux and the lack of a complete experimental set of data covering all scenarios of interest that limits the understanding of certain key aspects occurring in the process.

Various experimental campaigns, performed in different international laboratories, resulted in the evaluation of the dry deposition velocities for different types of pollutants and deposition surfaces. Nevertheless, there is a difficulty in generalizing this phenomenon because the velocity values differ by four orders of magnitude for gases and three orders of magnitude for particles (Sehmel, 1980; Pryor et al., 2007; Guha, 2008; Petroff et al., 2008). These issues limit the possibility of studying the dry deposition process using a single modeling approach. In fact, the models proposed in literature are not capable of representing dry deposition phenomena for several categories of pollutants and deposition surfaces because their applications is valid for specific conditions and if the data in that application meet all of the assumptions required of the data used to define the model.

In this field, some studies, performed at the Department of Energy, Information Engineering and Models Mathematicians (DEIM) of the University of Palermo, Italy, were focused on identifying of a approach capable of representing dry deposition phenomena for several categories of pollutants and deposition surfaces. Based on the study, a new scheme for the parameterization of the dry deposition velocity of particles is proposed. The primary goal is to develop a model that can be easily implemented within atmospheric dispersion modeling codes and is capable of efficiently addressing different deposition surfaces.

This study involved comparisons with experimental data reported in literature for different particle deposition scenarios. The results indicate that the proposed approach can determine, with good agreement, the main aspects of the phenomena involved in dry deposition processes for the studied environmental conditions and deposition surfaces.

* Corresponding author.
E-mail address: mariarosa.giardina@unipt.it (M. Giardina).

https://doi.org/10.1016/j.atmosenv.2018.02.038
Received 22 September 2017; Received in revised form 16 February 2018; Accepted 19 February 2018

2. Dry deposition process

The dry deposition process refers to all phenomena of meteorological, chemical and biological nature that influence a flux of gas and particle pollutants interacting with a ground surface without involving the water in the atmosphere.

In this field, the knowledge regarding the dry deposition of particles is far from complete due to the complex dependence of deposition on particle size, density, terrain, vegetation, meteorological conditions and chemical species.

The primary phenomena that are considered to affect the process can be described as follows:

- transport due to atmospheric turbulence in the low layer of the Planetary Boundary Layer (PBL), which is called the Surface Layer (SL). It is independent of the physical and chemical nature of the pollutant and depends only on the atmospheric turbulence level (i.e. turbulent movements of air);
- diffusion in the thin layer of air, which overlooks the air-ground interface (named the Quasi-Laminar Sublayer, QLS), where the molecular diffusion for gas, Brownian motion and turbulent diffusion for particles and gravity for heavier particles becomes dominant;
- transfer to the ground (e.g. interception, impaction, and rebound), which exhibits a pronounced dependence on the surface type with which the pollutant interacts.

The Brownian diffusion and eddy turbulence effects make a significant contribution to the total dry deposition velocity for particles in the size range from 0.01 μm to approximately a few micrometers. It is assumed to dominate the diffusion processes in the quasi-laminar sublayer surface. For particles of intermediate diameter d_p (in the range of approximately 0.1–1 μm), the process strongly depends on atmospheric conditions, surface characteristics, and particle size.

Above this range, the deposition is dominated by other phenomena, such as the inertial impaction characterized by the following interaction mechanisms (Petroff et al., 2008):

- Inertial impaction. If the particle inertia is too large, then the particle, transported by the flow towards an obstacle, cannot follow the flow deviation (particles may not be able to follow it due to inertia) and can consequently collide with the obstacle and remain on the surface.
- Turbulent impaction. In this mechanism, the particle has a sufficiently high velocity such that turbulent eddies can result in a transverse “free fight velocity”. Thus, particles possess sufficient momentum to reach the surface (Epstein, 1997; Almohammed and Breuer, 2016; Kor and Kharrat, 2016).

3. Short review of the dry deposition models for gas and particle

A key concept to studying the dry deposition process is the deposition velocity v_d (m s^{-1}) (i.e. the deposition velocity at a given height z), which can link the pollutant vertical flux to the concentration measured at quota z (m) to the ground reference level as follows:

$$v_d = \frac{F}{C(z)} \tag{1}$$

where F ($gm^{-2}s^{-1}$) is the pollutant flux removed per unit area; and $C(z)$ (gm^{-3}) is the pollutant concentration at quota z.

By considering that the reciprocal of v_d is the overall resistance to the mass transfer, the influence of the various phenomena on the deposition velocity can be expressed in terms of an electrical analogy. Based on the analogy of electrical circuits, the resistance to the deposition can be configured as resistances in circuits in parallel and series to describe the transfer factor between the air and the surface.

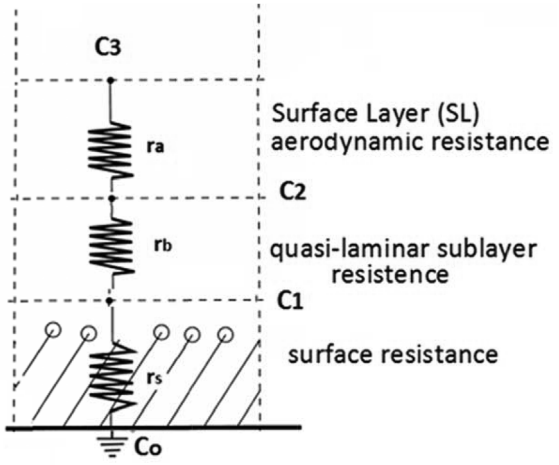

Fig. 1. Electrical analogy for the dry deposition of gaseous pollutants.

For a gaseous pollutant collection, it is possible to schematize the process, as indicated in Fig. 1; hence, we can express the relationship as follows:

$$\left|F\right| = \frac{C_3 - C_2}{r_a} = \frac{C_2 - C_1}{r_b} = \frac{C_1 - C_0}{r_s} \tag{2}$$

where r_a is the aerodynamic resistance considering the turbulence phenomenon in SL; r_b is the quasi-laminar sublayer resistance related to the diffusion phenomenon for gas and collisions due to the Brownian motion for particles; and r_s is the surface resistance, which depends on the nature of the receptor ground.

Based on the previous equation, the following relationship can be derived:

$$C_3 = (r_a + r_b + r_s)\,|F| \tag{3}$$

Accordingly, the dry deposition velocity formulation for gas can be given as follows:

$$v_d = \frac{1}{r_a + r_b + r_s} \tag{4}$$

Different studies have been reported in the literature (Wesely et al., 1985; Giorgi, 1986; Padro et al., 1991; Erisman et al., 1994; Padro, 1996; Wesely et al., 2001; Zhang et al., 2003; Kor and Kharrat, 2016) to evaluate parameters r_a and r_b. The calculation of the gas surface resistance r_s depends on the primary pathways for uptake, such as diffusion through the leaf stomata and uptake through the leaf cuticular membrane. A revised parameterization, which includes a realistic treatment of the cuticle and ground resistance in winter (low temperature and snow-covered surfaces) as well the handling of seasonally-dependent input parameters, has been reported in (Zhang et al., 2003).

For particle pollutants in the SL region, the turbulence acts on the particles’ motion similar to that on gas; however, the process is also influenced by gravity, so relationship Eq. (2) should be modified. In the quasi-laminar sublayer, as mentioned above, the deposition process is particularly influenced from the Brownian motion and the gravity due to heavier particles.

The resistances r_a, r_b and r_s are considered to be in parallel to a second pathway-gravitational settling, which can be defined as the reciprocal of the settling velocity (Slinn and Slinn, 1980; Hicks et al., 1985, 1987; Hanna et al., 1991; Seinfeld and Pandis, 1998).

Seinfeld and Pandis (1998) derived a dry deposition flux relationship based on the assumption that $r_s = 0$, which can be expressed by equating the vertical fluxes in two layers over a surface to the total resistance as follows:

$$\left|F\right| = \frac{C_3 - C_2}{r_a} + v_s c_2 = \frac{C_2 - C_1}{r_b} + v_s c_1 \tag{5}$$

The velocity v_d can be obtained by resolving the above equation as follows:

$$v_d = v_s + \frac{1}{r_a + r_b + r_a r_b v_s} \tag{6}$$

where the product $r_a\ r_b\ v_s$ represents a virtual resistance.

The settling velocity v_s increases in proportion to the square of the particle diameter, d_p, according to the law of Stokes, which is valid for particles with a diameter of up to 50 μm:

$$v_s = \frac{d_p^2\ g\ (\rho_p - \rho_a)\ C_c}{18\ \mu_a} \tag{7}$$

where g is the gravitational acceleration; ρ_p the particle density; ρ_a the air density; μ_a the air dynamic viscosity; and C_c the Cunningham factor (Seinfeld and Pandis, 1998). The parameter C_c can be given as follows:

$$c_c = 1 + \frac{\lambda_a}{d_p}\left(2{,}514 + 0{,}8\ e^{\frac{-0{,}55 d_p}{\lambda_a}}\right) \tag{8}$$

with λ_a mean free path of air.

As highlighted by Venkatram and Pleim (1999), the dry deposition velocity of particles based on the electrical analogy as described above are not consistent with the mass conservation equation. The vertical transport of particles can be modeled by assuming that the turbulent transport and particle settling can be added together as follows (Csanady, 1973):

$$K_p \frac{dC}{dz} + v_s C = F \tag{9}$$

where K_p is the eddy diffusivity for the mass transfer of species with a concentration C and v_s is the settling velocity evaluated from Eq. (7).

By integrating the above equation, it is possible to obtain the expression of the deposition velocity as follows:

$$v_d = \frac{v_s}{1 - e^{-[r(z)\ v_s]}} \tag{10}$$

where $r(z)$ is the total resistance to the transport, which can be computed as a function of d_p and height z (quota to the ground reference level), as explained in the following section.

It should be noted that there may be a slight difference between the magnitudes of the dry deposition velocities estimated using Eqs. (6) and (10) (Venkatram and Pleim, 1999).

4. New model for dry deposition of particles

A new scheme based on the electrical analogy is proposed, as indicated in Fig. 2.

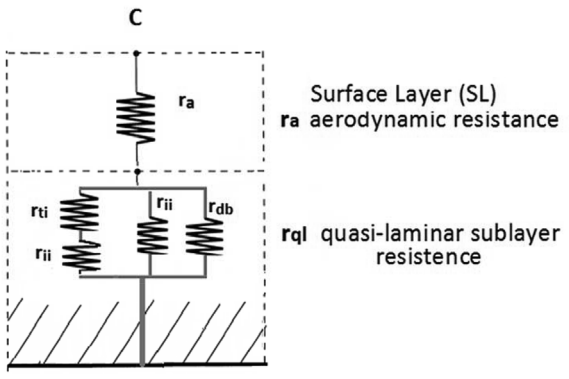

Fig. 2. New schematization for the parametrization of the deposition velocity for particles.

It is assumed that the resistances that affect the particle flux in the SL and QLS layers can be combined, as described below:

- aerodynamic resistance r_a (i.e. contribution to the deposition due to the atmospheric turbulence in the SL) is connected in series with the resistance r_{ql} across the quasi-laminar sublayer related to mechanisms of diffusion by Brownian motions and the impaction phenomena;
- quasi-laminar sublayer resistance r_{ql} is evaluated by considering a parallel circuit, as indicated in Fig. 2. The contribution of Brownian diffusion motions and the impaction phenomena can be considered as follows:
  1. r_{db} resistance considers the contribution of the Brownian diffusion;
  2. r_{ii} resistance contemplates the single effect of the inertial impaction regime for large particles;
  3. r_{ii} and r_{ti} resistances are connected in series to consider the specific local features of the mutual influence of the inertial impact processes (characterized by resistance r_{ii}) and the turbulent impact phenomena (characterized by resistance r_{ti}).

Accordingly, the total resistance r can be evaluated using the equation as follows:

$$r(z) = r_a + r_{ql} \tag{11}$$

The resistance r_a can be determined by using the Monin–Obukhov similarity theory which allows to obtain the relationship (Wesely and Hicks, 1977; Slinn et al., 1978; Hicks, 1982; Voldner et al., 1986; Hanna et al., 1991; Baldocchi et al., 1995; Maryon et al., 1996; Seinfeld and Pandis, 1998):

$$r_a = \frac{1}{k u_*}\left(ln\frac{z}{z_o} - \Psi_h\right) \tag{12}$$

where u_* is the friction velocity, which represents the intensity of the atmospheric turbulence; z_o is the surface roughness height above the displacement plane; and k is the von Karman constant (generally equal to 0.4).

Brandt et al. (2002) suggested the following relationships for calculating parameter Ψ_h in Eq. (12):

$$\Psi_h = -5\frac{z}{L} \quad \text{with } \frac{z}{L} > 0 \text{ (stable atmospheric conditions)} \tag{13}$$

$$\Psi_h = e^{\left\{0{,}598 + 0{,}390\ ln\left(-\frac{z}{L}\right) - 0{,}09\left[ln\left(-\frac{z}{L}\right)\right]^2\right\}} \quad \text{with } \frac{z}{L} < 0 \text{ (unstable atmospheric conditions)} \tag{14}$$

where L is the Monin-Obukhov length, which can be computed as follows:

$$L = \frac{u_*^3 c_p \rho \overline{T}}{kgH} \tag{15}$$

where c_p is the specific heat at constant pressure; $\overline{T}$ the average temperature in SL; and H the sensible heat.

Based on the above hypotheses, the resistance r_{ql} is evaluated as follows:

$$\frac{1}{r_{ql}} = \left(\frac{1}{r_{db}} + \frac{1}{r_{ii}} + \frac{1}{r_{ii} + r_{ti}}\right) \tag{16}$$

Various models in literature predict a functional dependence of the resistance related to Brownian diffusion phenomena, r_{db}, on the Schmidt number, Sc. A general expression can be stated as follows:

$$r_{db} = \frac{1}{u_*} c\ Sc^p \tag{17}$$

where c and p are constant and Sc is evaluated as:

$$Sc = \frac{\nu_a}{D} \tag{18}$$

where ν_a is the air kinematic viscosity ($m^2\ s^{-1}$), and D is the particle's Brownian diffusivity of air ($m^2\ s^{-1}$) determined from Stokes-Einstein equation:

$$D = \frac{K_B T C_C}{3\pi\mu_a d_p} \tag{19}$$

with K_B the Boltzmann constant (J/K); T the absolute temperature; μ_a the air dynamic viscosity; and C_C the Cunningham factor from Eq. (8).

The parameter p in Eq. (17) usually lies between 1/2 and 2/3 with larger values for rougher surfaces. For example, Slinn and Slinn (1980) suggested a value of 1/2 for water surfaces, and Slinn (1982) proposed a value of 2/3 for vegetated surfaces. Zhang et al. (2001) used values of p varying with land use categories.

In this study, for all surface conditions the following relationship is assumed:

$$r_{db} = \frac{1}{u_* Sc^{-2/3}} \quad \text{for all surface conditions} \tag{20}$$

The transport of particles by the Brownian diffusion represented by Eq. (20) is recommended in various studies on the basis of theoretical and empirical results (Wesely and Hicks, 1977; Paw, 1983; Hicks et al., 1987; Pryor et al., 2009; Bae et al., 2009; Kumar and Kumari, 2012).

The resistance for the inertial impact process r_{ii} is evaluated using the relationships valid for smooth and rough surfaces:

$$r_{ii} = \frac{1}{u_*\left(\frac{St^2}{St^2+400}\right)} \quad \text{for smooth surfaces} \tag{21}$$

$$r_{ii} = \frac{1}{u_*\left(\frac{St^2}{St^2+1}\right)} \quad \text{for rough surfaces} \tag{22}$$

where St is the Stokes number defined as:

$$S_t = \frac{v_s}{g}\frac{u_*^2}{\nu_a} \tag{23}$$

with v_s the settling velocity from Eq. (7).

Various authors suggested these or similar formulae for the impaction efficiency as a function of smooth surfaces and surfaces with rough elements (Slinn, 1982; Giorgi, 1986; Peters and Eiden, 1992). For example, Zhang et al. (2001) proposed impaction efficiency characterized by relationship varying with the land use cover.

The resistance related to turbulent impact phenomena r_{ti} is predicted as a function of dimensionless particle relaxation time, τ_+, as follows:

$$r_{ti} = \frac{1}{u_* m \tau_+^n} \quad \text{all surfaces} \tag{24}$$

where τ_+ is evaluate using the following relationship:

$$\tau_+ = \tau\frac{u_*^2}{\nu_a} \tag{25}$$

with τ the particle relaxation time defined for a spherical particle as follows:

$$\tau = \frac{d_p^2 \rho_p C_c}{18\mu_a} \tag{26}$$

For turbulent deposition in pipe flows, the following regimes have been observed (Guha, 1997, 2008):

- Regime with approximately $\tau_+ < 0.1$ (very small particles): Brownian diffusion becomes significant and deposition is affected by a combination of the Brownian and eddy diffusions. For the Brownian regime, the deposition velocity is a function of the Schmidt number.
- Regime with approximately $0.1 < \tau_+ < 30$: particle motion is strongly dependent on the turbulent fluctuation in the fluid flow, and the deposition velocity increases with τ_+. For larger particles, the deposition velocity can be considered to be proportional to a second power of τ_+.
- Regime with approximately $\tau_+ > 30$: particles have large inertia, and the effects of turbulence on the particle motion are significantly reduced; furthermore, the gravity effect is dominant.

For most trace gases, the uncertainty associated with the value of the exponent n is not critical; however, for extremely slowly diffusing quantities, such as aerosol particles, the uncertainties become large. This phenomenon remains a subject to be further studied.

In this study, the constants m and n in Eq. (24) have been determined by adapting Eqs. (10), (16), (20), (21) and (24) to the experimental data reported in (Chamberlain, 1967; Liu and Agarwal, 1974). The authors experimentally investigated the deposition of aerosol particles for comparable values of friction speeds. The fitting procedure determines the values of the constants m and n to be 0.1 and 3, respectively.

In the light of the above considerations, Eq. (10) can be evaluate as follows:

$$v_d = \frac{v_s}{1 - e^{-\left\{v_s\left[r_a+1\,/\left(\frac{1}{r_{db}}+\frac{1}{r_{ii}}+\frac{1}{r_{ii}+r_{ti}}\right)\right]\right\}}} \tag{27}$$

where r_a, r_{db} and $r_{ti}$are evaluated using Eq.s (12), (20), and (24), in which the constants m = 0.1 and n = 3 are used. The parameter $r_{ii}$is evaluated using Eq.s (21) or (22) for smooth or rough surfaces, respectively.

5. Comparison with experimental data and other dry deposition models

The new model for computing the deposition velocity v_d is validated through a comparison with several experimental data reported in the literature depending on the particle diameter, d_p, for different meteorological conditions and surface typologies, such as short grass, grassland, sand, forest and water in its liquid phase. Unless otherwise stated, the particle density is selected as 1000 ($kg\ m^{-3}$).

Moreover, comparisons against results obtained by using models that are widely applied to study dry deposition process to different type of surfaces are also shown.

Additionally, the settling velocity v_s evaluated using Eq. (7) is depicted in a few of the figures described in the following section.

5.1. Deposition on smooth surfaces

The deposition velocity for smooth surface is calculate using Eq. (27), where the parameter r_{ii} is evaluated from Eq. (21).

Fig. 3 illustrates a comparison among predictions of deposition speed v_d, obtained using the proposed model for friction velocities of $u_* = 0.75$ and 0.26 ($m\ s^{-1}$); experimental measurements reported in (Liu and Agarwal, 1974) and (Chamberlain, 1967) for grass and sticky artificial grass, respectively; and experimental data reported in (Pellerin et al., 2017) for grassland. CFD simulations reported in (Tang et al., 2015), relevant to certain data from Liu and Agarwal (1974), are also illustrated. Additionally, predictions using models of Zhang et al. (2001) and Slinn (1982) for $u_* = 0.26$ ($m\ s^{-1}$) are reported for the purposes of comparison with some theoretical approaches most in use at present. In this last case, the deposition speed is modeled for stable atmospheric conditions, particle density of 2650 ($kg\ m^{-3}$) and roughness length $z_0 = 0.02$ (m), as suggested in (Pellerin et al., 2017).

Fig. 4 presents the comparisons among the predictions obtained for friction velocities of $u_* = 0.341$ and 0.114 ($m\ s^{-1}$), and the experiments

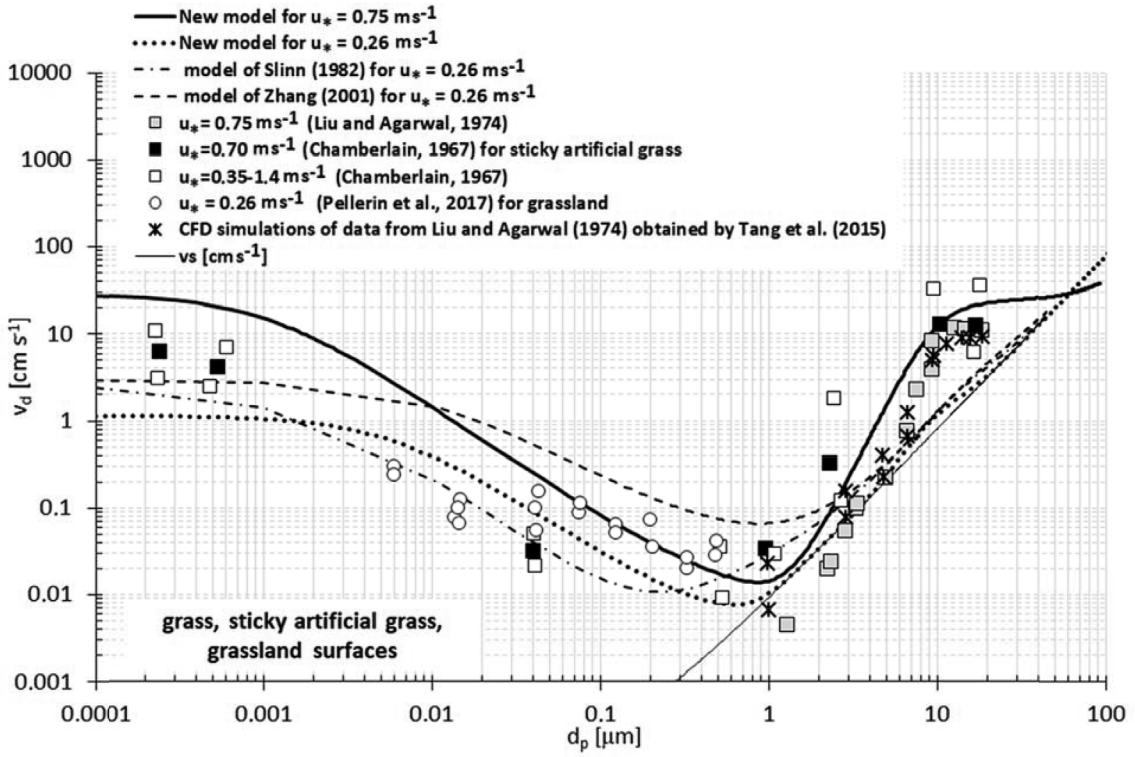

Fig. 3. A comparison between deposition velocity predictions, obtained using the new model for friction velocities $u_* = 0.75$ and 0.26 (m s^{-1}), and experimental measurements reported in (Chamberlain, 1967; Liu and Agarwal, 1974; Pellerin et al., 2017). CFD simulations of experimental data from Liu and Agarwal (1974), as reported in (Tang et al., 2015), are depicted. Additionally, predictions using the models of Slinn (1982) and Zhang et al. (2001) are shown for $u_* = 0.26$ (m s^{-1}).

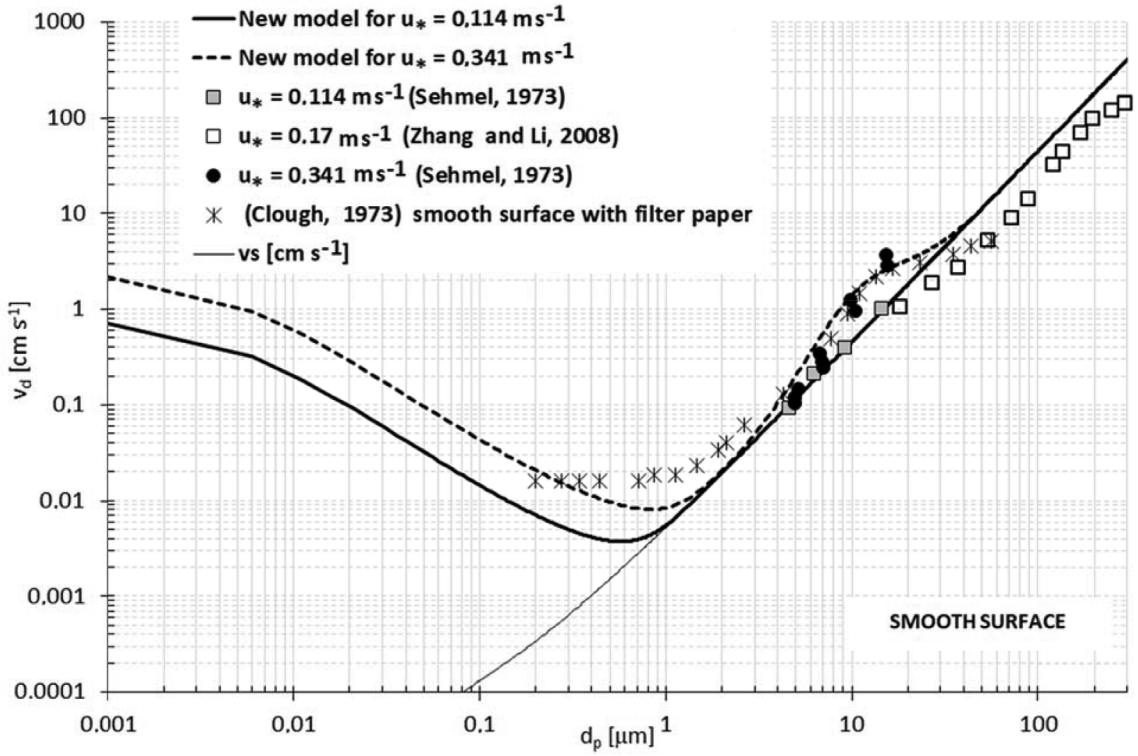

Fig. 4. A comparison between the deposition velocity predictions obtained using the new model and the experimental measurements reported in (Sehmel, 1973) for smooth floor surfaces. Additionally, the data obtained by Zhang and Li (2008) for friction velocity $u_* = 0.17$ (m s^{-1}) and experiments reported in (Clough, 1973), valid for smooth surfaces with filter paper, are depicted.

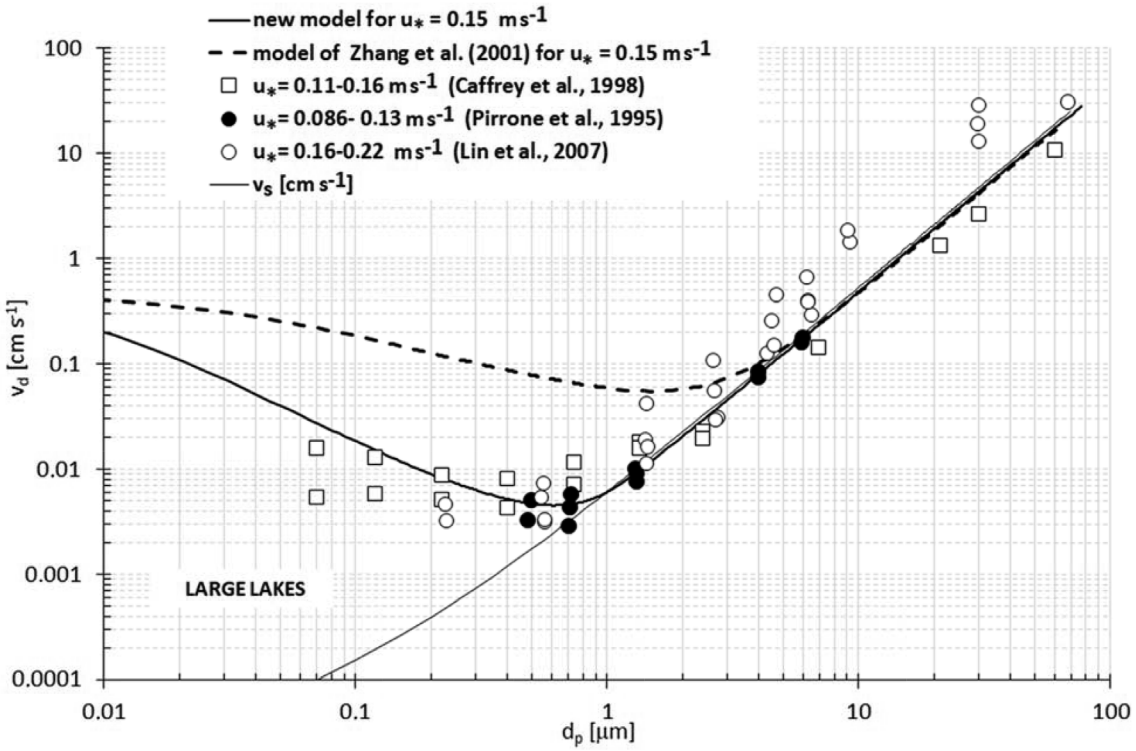

Fig. 5. A comparison between the deposition velocities obtained using the new model with a friction velocity $u_* = 0.15$ (m s^{-1}) and the experimental data reported in (Pirrone et al., 1995; Caffrey et al., 1998; Lin et al., 2007) for large lakes and similar values of u_*. The predictions obtained using the model of Zhang et al. (2001) are shown.

reported in Sehmel (1973), which are valid for smooth floors. Furthermore, for a comparison among experiments with similar deposition surfaces, the experimental data obtained by (Clough, 1973) are reported. Data obtained by Zhang and Li (2008) with a nominal friction velocity of $u_* = 0.17$ (m s^{-1}) are also shown. These authors highlighted that their data exhibit a similar slope of the experiments collected by Sehmel (1973) at a friction velocity of 0.114 (m s^{-1}).

Fig. 5 through 7 present comparisons of dry deposition velocity predictions and experiments relevant to large lakes and water surfaces. The results obtained using the model of Zhang et al. (2001) for some values of the friction velocity are reported.

In particular, Fig. 5 shows experiments obtained by Caffrey et al. (1998) for the dry deposition on large lakes. For a comparison among experimental data with the same deposition surface and similar friction velocities, the data obtained by Pirrone et al. (1995) and Lin et al. (2007) are also reported.

For water surface, Fig. 6 presents experimental data obtained by Sehmel and Sutter (1974) using a high friction velocity of $u_* = 1.17$ (m s^{-1}), results obtained using the models of Slinn and Slinn (1980) and Zhang et al. (2001) are also reported.

Fig. 7 depicts the experimental measurements reported in (Möller and Schumann, 1970) and (Sehmel and Sutter, 1974) using friction velocities of $u_* = 0.4$ and 0.44 (m s^{-1}), respectively. Additionally, the experimental data reported in (Sehmel and Sutter, 1974; Zufall et al., 1998), obtained using similar atmospheric conditions, are also shown. The predictions evaluated using the model of Zhang et al. (2001) are shown for $u_* = 0.11$ (m s^{-1}).

5.2. Deposition on rough surfaces

The deposition velocity for rough surface is calculate using Eq. (27), where the parameter r_{ii} is evaluated from Eq. (22).

The results are reported in Fig. 8 through 13 for different rough canopies. Moreover, the predictions obtained using the model of Zhang et al. (2001) for forest, plant and sticky wood surfaces are shown in Fig. 8 through 10, as well as in Fig. 13.

In particular, Fig. 8 reports comparisons between the deposition velocity predictions and the experimental data obtained by Pryor et al. (2007, 2009), for forest land use and two different values of friction speed.

A further comparison has been performed using the experimental measurements reported in (Zhang et al., 2014) for several surface typologies. In particular, Fig. 9 reports the comparison for "sticky wood", Fig. 10 for "plant", Figs. 11 and 12 for "sand" and "sandy loam", respectively. In Fig. 10, for a comparison among experimental data with similar surfaces, the data obtained by (Hofken and Gravenhorst, 1982; Grönholm et al., 2007; Pryor et al., 2007) are also depicted.

In Table 1, the values of the friction speed u_* and roughness z_0 used in Zhang's experimental tests are reported. It should be noted that the authors reveal the uncertainties for the experimental data, which is especially significant for d_p values less than about 10 µm (Zhang et al., 2014).

Finally, Fig. 13 reports the experiments obtained by Pellerin et al. (2017) for bare soil (campaigns performed in March 2008), maize (campaigns performed in June 2007 and 2008) and forest (campaigns performed in south-west France; July 2014). A comparison with the model proposed by Slinn (1982) is added.

5.3. Results and discussion

The performance of the dry deposition velocity model has been compared to a number of experiments for smooth (Fig. 3 through 7) and rough surfaces (Fig. 8 through 13), as well as with other models that have been adopted in a large number of studies and applications, i.e. the models of Slinn and Slinn (1980, 1982) and Zhang et al. (2001).

Slinn and Slinn (1980) proposed a detailed model for deposition to water surfaces. The model of Slinn (1982) is considered a model that predicts adequately the particle deposition on grass or low-roughness canopies (Gallagher et al., 2002), while the model of Zhang et al. (2001) is particularly suited for predicting the fine particle depositions

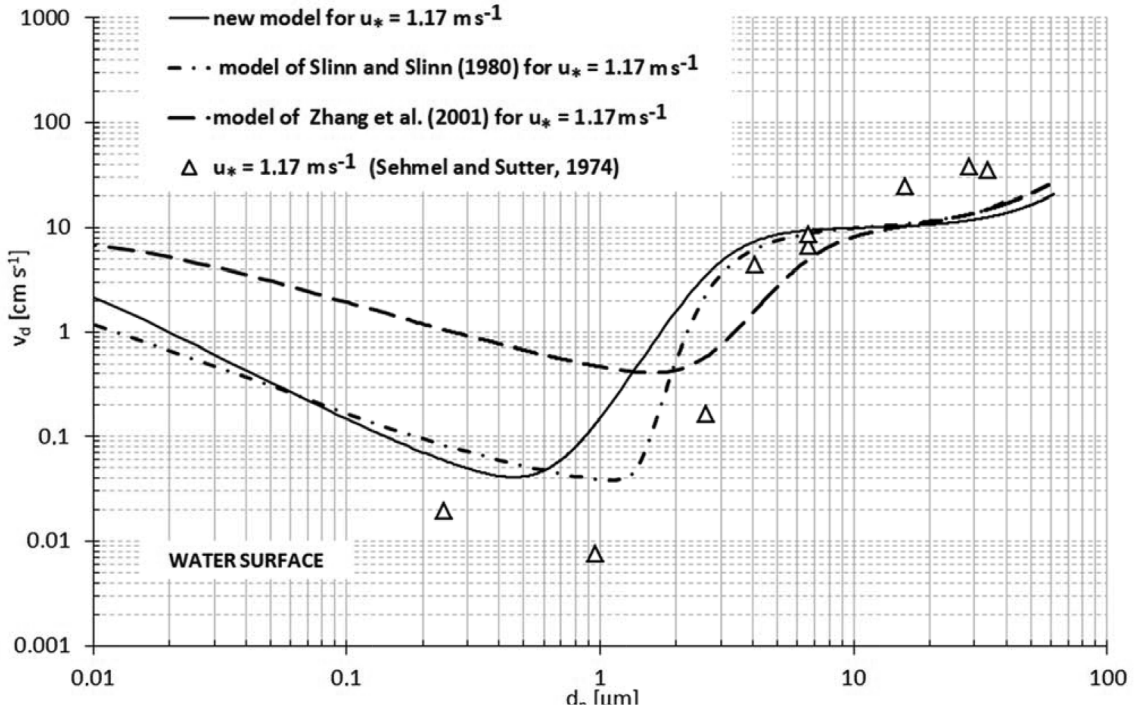

Fig. 6. Predictions obtained using the new model are compared against experimental data obtained by Sehmel and Sutter (1974) for water surfaces with a friction velocity of $u_* = 1.17$ (m s^{-1}). The results obtained using the models of Slinn and Slinn (1980) and Zhang et al. (2001) are reported for the same friction velocity.

on highly rough surfaces, such as forest (Petroff et al., 2008). However, on other surfaces, their results do not agree as well with measurements and differences more than of one order of magnitude can arise (Petroff et al., 2008).

On the whole, the proposed model produces results in accordance with a large number of measurements, allowing predictions that are sufficiently accurate and sensitive to the change of canopy. On this point, let us say that this result is being achieved by accounting different parametrization of inertial impact processes for smooth and rough surfaces by using the resistances described by Eqs (21) and (22),

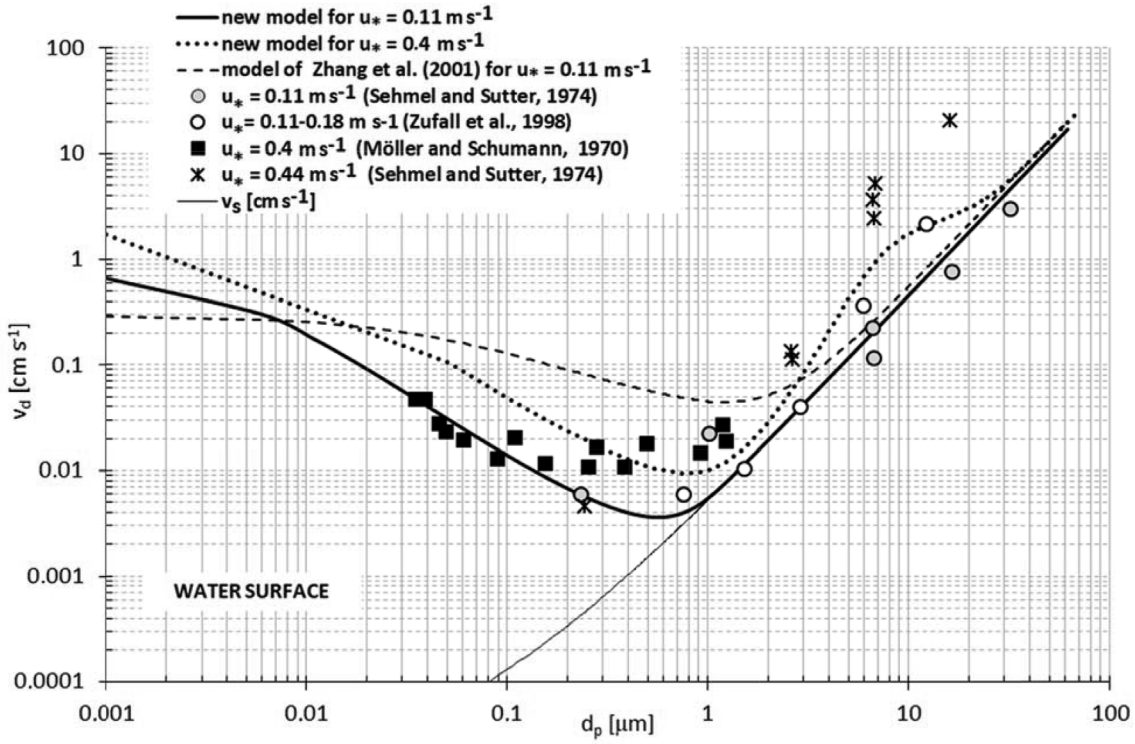

Fig. 7. A comparison between the deposition velocity predictions, obtained using the new model, and the experimental measurements reported in (Möller and Schumann, 1970; Sehmel and Sutter, 1974) for water surfaces. Additionally, the experimental data reported in (Sehmel and Sutter, 1974; Zufall et al., 1998) for similar values of the friction velocity are depicted. The predictions evaluated using the model of Zhang et al. (2001) are shown for $u_* = 0.11$ (m s^{-1}).

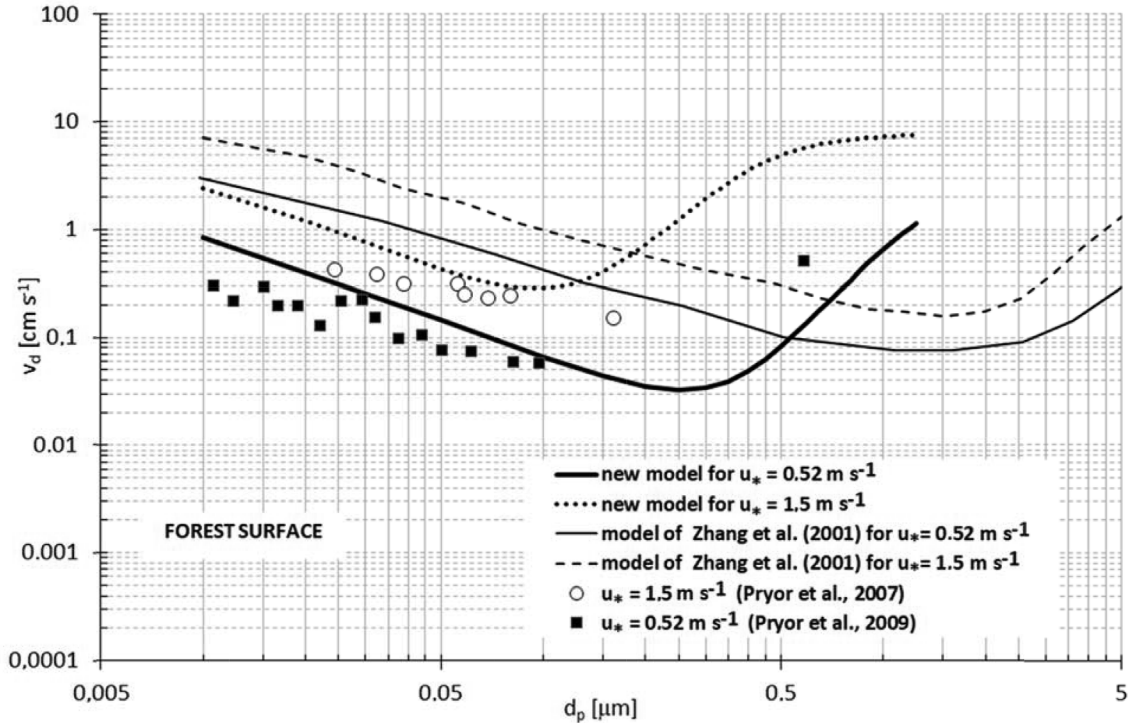

Fig. 8. A comparison between the deposition velocities evaluated using the new model and the experimental data obtained by Pryor et al. (2007, 2009) for forest surfaces. The results obtained using the model of Zhang et al. (2001) are shown for the same friction velocities.

respectively. Additionally, in the turbulent-impaction regime, a sharp increase of the deposition velocity is noticeable, despite a variability of the results, and denotes a strong influence respect to the particle inertia. The combination of the resistances r_{ii} and r_{ti}, as described in section 400000, allows to catches this phenomenon, improving the predictions especially for coarse particles.

For smooth surfaces (Fig. 3 through 7), it should be noted that the model correctly predicts the minimum value of deposition velocity for a particle diameter of about 1 µm, except for friction velocity as high as 1.17 (m s^{-1}) (Fig. 6).

Fig. 3 shows experimental data valid for dry deposition processes to grass and grassland surfaces. The proposed model for $u_* = 0.26$ (m s^{-1})

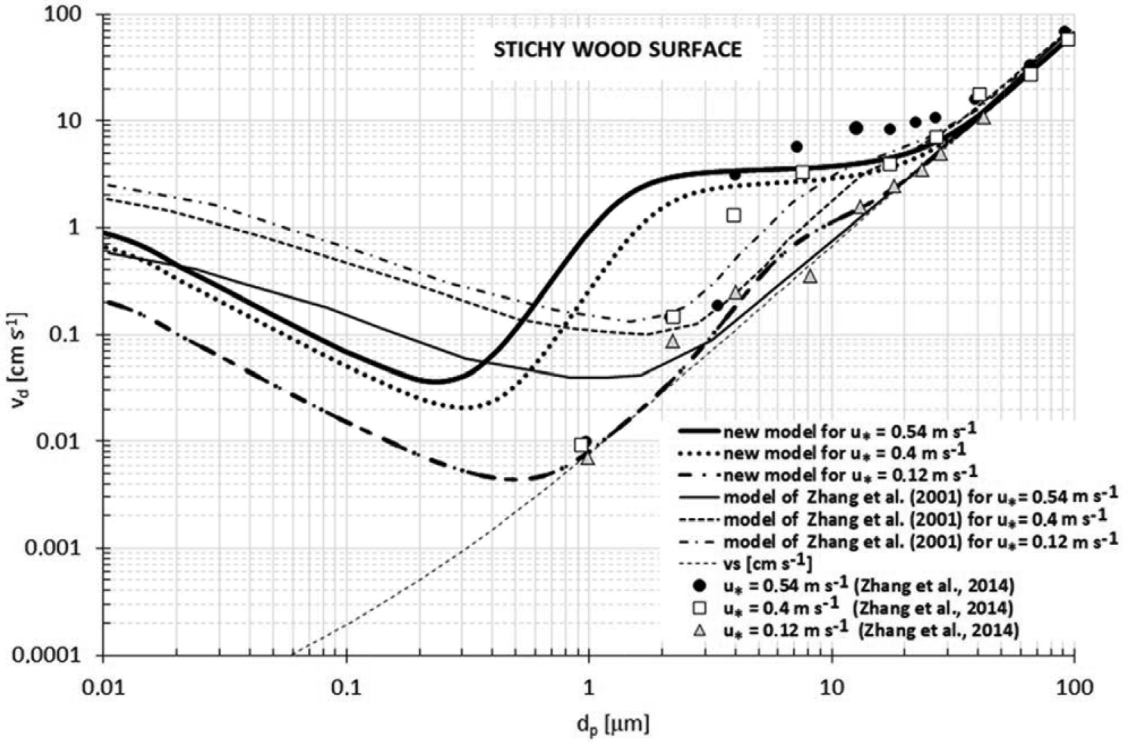

Fig. 9. A comparison between deposition velocity predictions and experimental data obtained by Zhang et al. (2014) for sticky wood surface. The results obtained using the model of Zhang et al. (2001) are shown for the same friction velocities.

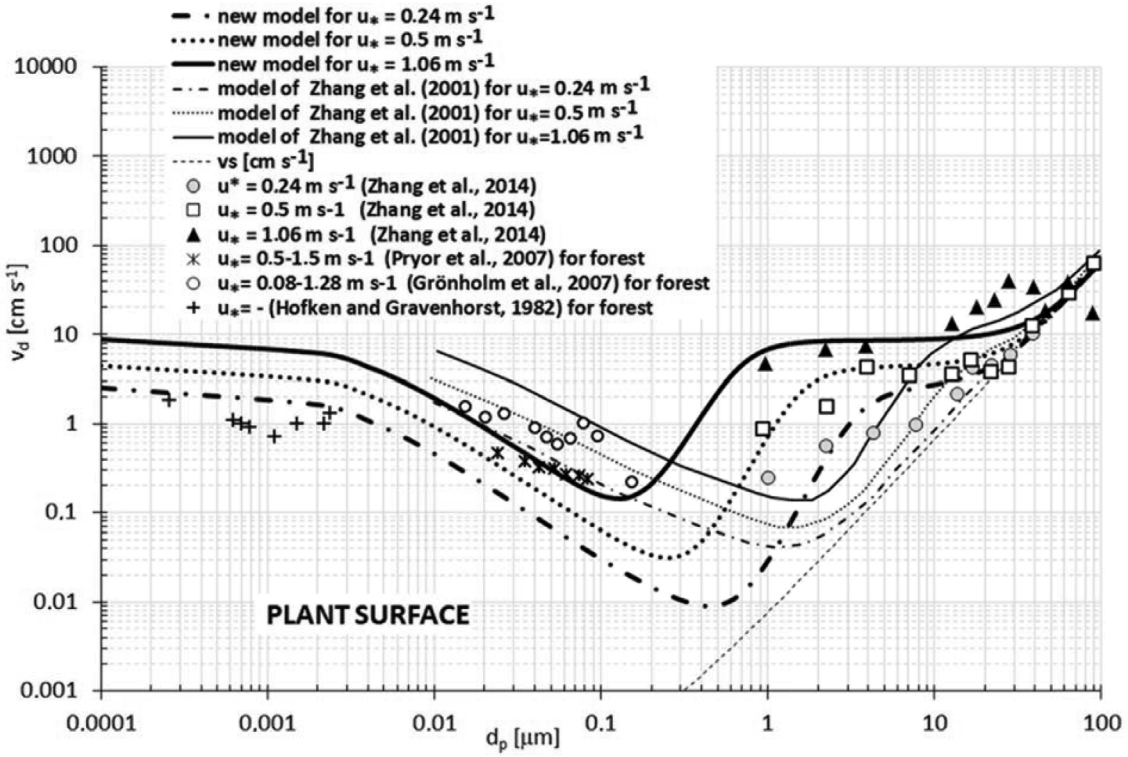

Fig. 10. A comparison between the deposition velocities evaluated using the new model and the experimental data obtained by Zhang et al. (2014) for plant surfaces. The results obtained using the model of Zhang et al. (2001) for the same friction velocities are shown. For a comparison among experiments characterized by similar test conditions, the data reported in (Hofken and Gravenhorst, 1982; Pryor et al., 2007; Grönholm et al., 2007) are depicted.

is close to one of Slinn (1982) and both allow a good agreement with the experiments reported in (Pellerin et al., 2017) for d_p below 1 μm. The experimental data reported for $u_* = 0.7$ and 0.75 (m s^{-1}) show that the impaction process is predominant respect the gravitational effects, this can be deduced from data which are situated over the v_s curve representing the gravitational settling velocity trend (thin line). This aspect is captured by the proposed approach and CFD simulations reported in (Tang et al., 2015).

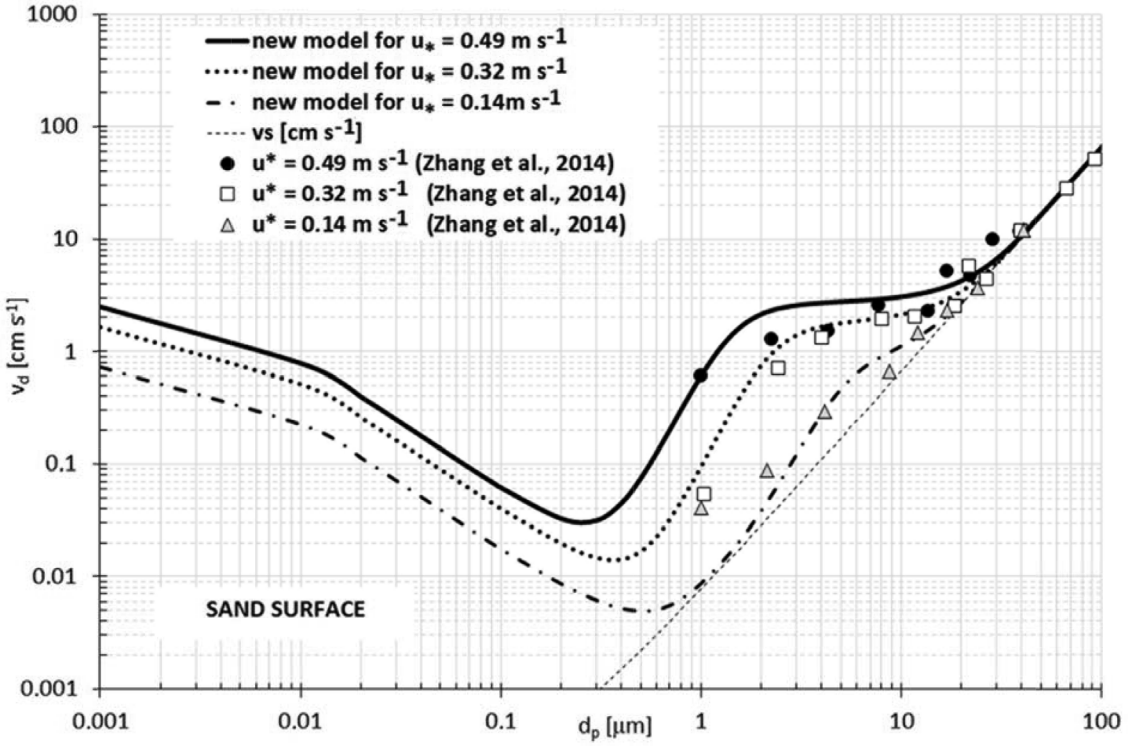

Fig. 11. A comparison between the deposition velocity predictions and the experimental data obtained by Zhang et al. (2014) for sand surfaces.

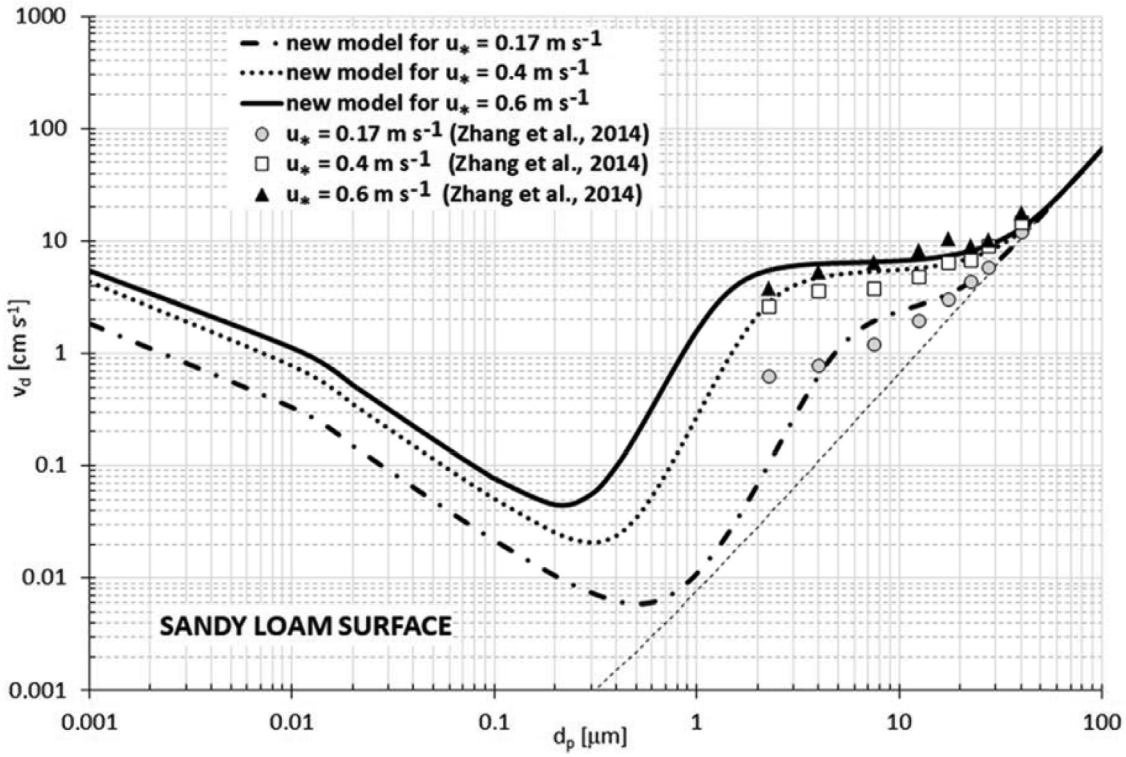

Fig. 12. A comparison between the deposition velocity predictions and the experimental data obtained by Zhang et al. (2014) for sandy loam surfaces.

Table 1
Data used for the validation of the model with the experimental measurements reported in (Zhang et al., 2014).

	u* (m/s)	z_0 (mm)
Sticky wood	0.12	0.075
	0.40	0.033
	0.54	0.032
Sand	0.14	0.153
	0.32	0.143
	0.49	0 135
Plant	0.24	5.927
	0.50	2.877
	1.06	2.106
Sandy loam	0.17	0.85
	0.40	0.84
	0.30	0.68

As regards the results of smooth surfaces reported in Fig. 4, the proposed model allows a good agreement with experimental data and the effect due to impaction process is predicted by using a friction velocity of $u_* = 0.341$ (m s^{-1}).

Some interesting insights can be withdrawn by a review of the results relevant to water surface, reported in Fig. 5 through 7. In Figs. 6 and 7 the experiments reported in (Möller and Schumann, 1970; Sehmel and Sutter, 1974) are obtained from water/wind tunnel measurements. In these conditions Slinn et al. (1978) highlighted that for particles smaller than approximately 0.1 μm, an increase in v_d for an increasing diffusivity given by an $Sc^{2/3}$ dependence may be correct. Additionally, for particles higher than approximately 1 μm, v_d can be larger than the gravitational settling speed. This phenomenon may be caused by an increase in the inertial impaction on waves (Sehmel, 1973). Similar considerations can be made for large lakes surfaces (Fig. 5). The trend of v_d obtained using the proposed model appears to capture this phenomenon only when the friction velocity of $u_* = 0.3$ (m s^{-1}), or higher, is used (see Figs. 6 and 7).

Comparisons against predictions obtained using other models of Fig. 6 show that the proposed model is close to the one of Slinn and Slinn (1980), and both show an overestimation of experiments up to particle diameter of $d_p = 2$ μm. However, the model of Slinn and Slinn (1980) allows a better prediction of the minimum of the deposition velocity (d_p of about 1 μm). The Zhang's model shows an overestimation of experimental data (two order of magnitude) if the particle diameter is below of about $d_p = 2$ μm; above this value it results very close with the other two models and the experiments.

Also for rough surfaces, overall good agreement between the simulated trends of v_d and the experiments can be found. However, the comparison between the proposed model and the experimental data reported in Fig. 9 highlighted an overestimation by a factor of 10 for the test relevant to "sticky wood" surfaces for $u_* = 0.4$ (m s^{-1}) and d_p value lower than 3 μm.

The predictions obtained using the Zhang's model for forest surface (Fig. 8) show an overestimation respect to the experiments. This result indicates that the contribution from Brownian diffusion is underestimated. Moreover, Zhang's model for deposition to sticky wood and plant surfaces, reported in Figs. 9 and 10, show differences more than of one order of magnitude for d_p value lower than 10 μm.

Finally, Fig. 13, where a comparison between the simulated deposition velocities, normalized by $u_* = 0.26$ (m s^{-1}), and experimental measurements reported in (Pellerin et al., 2017) are reported, shows a good agreement in trend.

On the basis of all results, three noticeable features can be observed using the proposed model: first, a minimum of the deposition velocity is predicted in most examined experiments. Second, the model is consistent with the behaviour recommended according to the physical meaning of the deposition processes. Finally, the validation work indicates that the model, applied for smooth surface, is usable if conditions with roughness length z_0 in the range 10^{-5} through 0.02 (m) are examined, for rough surfaces the model is usable if z_0 is in the range 0.03 through 6 (m).

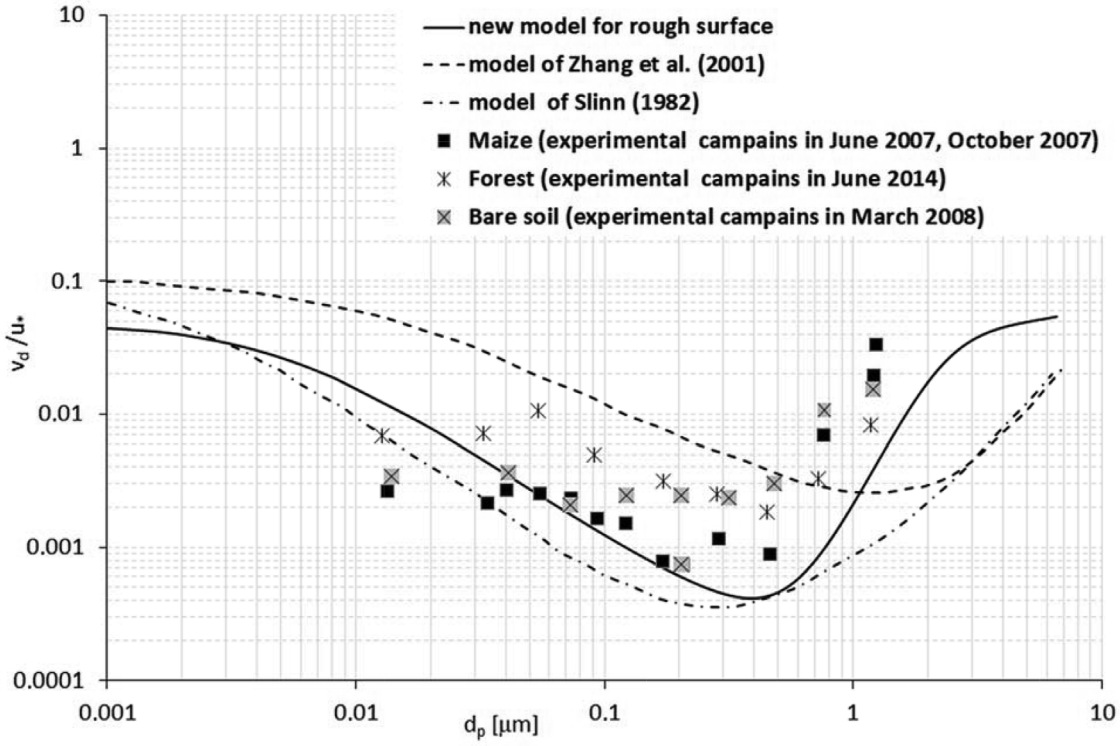

Fig. 13. A comparison between predictions of deposition velocities normalized by $u_* = 0.26$ (m s^{-1}) and experimental measurements reported in (Pellerin et al., 2017) for bare soil, maize and forest. Additionally, the results using the models of Zhang et al. (2001) and Slinn (1982) are shown for the same friction velocity.

6. Conclusion

The ATMES (Atmospheric Transport Model Evaluation Study) report, which is relevant to the study of models that evaluate radioactive pollutants dispersed in the ambient atmosphere, highlighted that the highest uncertainties are in the parametrization of the source terms and the dry and wet deposition velocities (Klug et al., 1992).

There are several models found in the literature; however, none are able to exhaustively address most of the phenomenology related to pollutant deposition because of the numerous complex involved processes. A review of the existing mechanistic models emphasizes the wide variety in which captation occurs; however, a comparison of two similar scenarios results in large discrepancies, i.e. two orders of values are obtained for the same particle diameter.

As highlighted by Sehmel (1980), the measurements of the deposition velocity performed by different international laboratories do not allow general conclusions to be drawn due to experimental uncertainness.

A bibliographical study of the experimental tests performed to evaluate the dry deposition velocities for a vegetative canopy (i.e. experiment in situ) or derived by wind tunnel measurements demonstrates a substantial number of differences that are more pronounced for forest canopies or in the accumulation range.

For the same pollutant typology, the experimental data indicates that for gas, the values of the deposition velocity differ by as much as four orders of magnitude for gas and up to three orders of magnitude for particles.

The primary goal of our study was to develop an approach that could be easily implemented within atmospheric dispersion modeling codes and be capable of efficiently addressing different deposition surfaces for several radioactive pollutants. The parametrizations reported in literature can be applied for multiple size classes (i.e. particle diameter) or based on several assumptions, which may be frequently violated in practice (Pryor et al., 2009). Furthermore, they may even be strongly dependent on several parameter combinations, such as land use classification and seasonal categories.

In this paper a new model for the deposition velocity of particles based on an electrical analogy was proposed to modify the parametrization of laminar sublayer resistances. The obtained relationships are obtained by assuming that the resistances that affect the particle flux in the Quasi-Laminar Sublayers can be combined to take into account local features of the mutual influence of inertial impact processes and the turbulent one.

The validation study, which was conducted using a significant number of experimental data collected from literature, allowed the goodness of the proposed approach to be verified.

Further studies concerning the integration of phenomena such as rebound, which influence coarse particle depositions (size typically larger than 5 μm), and the interception by obstacles should be performed.

References

Almohammed, N., Breuer, M., 2016. Modeling and simulation of particle-wall adhesion of aerosol particles in particle-laden turbulent flows. Int. J. Multiphas. Flow 85, 142–156.
Bae, S.Y., Jung, C.H., Kim, Y.P., 2009. Development of an aerosol dynamics model for dry deposition process using the moment method. Aerosol. Sci. Technol. 43 (6), 570–580.
Baldocchi, D.D., Paw, K.T., Shaw, R.H., Snyder, R.L., 1995. Advanced Short Course on Biometeorology and Micrometeorology. 26 Giugno – 1 Luglio 1995, Sassari, Italia.
Brandt, J., Christensen, J.H., Frohn, L.M., 2002. Modelling transport and deposition of caesium and iodine from the Chernobyl accident using the DREAM model Atmos. Chem. Phys. 2, 397–417.
Caffrey, P., Ondov, J., Zufall, M., Davidson, C., 1998. Determination of size-dependent dry particle deposition velocities with multiple intrisic elemental tracers. Environ. Sci. Technol. 32, 1615–1622.
Chamberlain, A.C., 1967. Transport of Lycopodium spores and other small particles to rough surfaces. Proc. Roy. Soc. Lond. A 296, 45–70.
Clough, W.S., 1973. Transport of particles to surfaces. J. Aerosol Sci. 4, 227–234.
Csanady, G.T., 1973. Turbulent Diffusion in the Environment. Reidel, Dordrecht, Holland.
Epstein, N., 1997. Elements of particle deposition onto nonporous solid surfaces parallel to suspension flows. Exp. Therm. Fluid Sci. 14 (4), 323–334.
Erisman, J.W., Van Pul, A., Wyers, G.P., 1994. Parameterization of surface resistance for the quantification of atmospheric deposition of acidifying pollutants and ozone. Atmos. Environ. 28, 2595–2607.

Gallagher, M.W., Nemitz, E., Dorsey, J.R., Fowler, D., Sutton, M.A., Flynn, M., Duyzer, J.H., 2002. Measurements and parameterisations of small aerosol deposition velocities to grassland, arable crops, and forest: influence of surface roughness length on deposition. J. Geophys. Res. 107, 287–292.
Giorgi, F., 1986. A particle dry deposition parameterization scheme for use in tracer transport models. J. Geophjx Res. 91, 9794–9806.
Grönholm, T., Hiltunen, V., Aalto, P.P., Laakso, L., Rinne, J., coauthors, 2007. Measurements of aerosol particle dry deposition velocities using relaxed eddy accumulation technique. Tellus 59, 381–386.
Guha, A., 1997. A unified eulerian theory of turbulent deposition to smooth and rough surfaces. J. Aerosol Sci. 28 (8), 1517–1537.
Guha, A., 2008. Transport and deposition of particles in turbulent and laminar flow. Annu. Rev. Fluid Mech. 40, 311–341.
Hanna, S.R., Gifford, F.A., Yamartino, R.J., 1991. Long range radioactive plume transport simulation model/code – phase I. In: USNRC Division of Contracts and Property Management, Contract Administration Branch, P-902, Washington, DC 20555. Technical Report.
Hicks, B.B., 1982. Critical assessment document on acid deposition, ATDL Contributory file 81/24. In: Atmospheric Turbulence and Diffusion Laboratory, NOAA, Oak Ridge, Tennessee.
Hicks, B.B., Baldocchi, D.D., Hosker, R.P., Hutchison, B.A., Matt, D.R., McMillen, R.T., Satterfield, L.C., 1985. On the Use of Monitores Air Concentrations to Infer Dry Deposition. NOAA Technical Memorandum ERLO ARLZ141.
Hicks, B.B., Baldocchi, D.D., Meyers, T.P., Hosker Jr., R.P., Matt, D.R., 1987. A preliminary multiple resistance routine for deriving dry deposition velocities from measured quantities. Water Air Soil Pollut. 36, 311–330.
Hofken, K.D., Gravenhorst, G., 1982. Deposition of atmospheric aerosol particles to beech- and spruce forest. In: Georgii, H.W., Pankrath, J. (Eds.), Deposition of Atmospheric Pollutants. D. Reidel Publishing Company, Oberursel/Taunus, Germany, pp. 191–194.
Klug, W., Graziani, G., Grippa, G., Pierce, D., Tassone, C., 1992. Evaluation of Long Range Atmospheric Transport Models Using Environmental Radioactivity Data from the Chernobyl Accident. Elsevier Applied Science, London and New York The ATMES Report.
Kor, P., Kharrat, R., 2016. Modeling of asphaltene particle deposition from turbulent oil flow in tubing: model validation and a parametric study. Petroleum 2 (4), 393–398.
Kumar, R., Kumari, K.M., 2012. Experimental and parameterization method for evaluation of dry Deposition of S Compounds to natural surfaces. Atmos. Clim. Sci. 2, 492–500.
Lin, J.J., Kenneth, E.N., Holsen, T.M., 2007. Dry deposition velocities as a function of particle size in the ambient atmosphere. Aerosol. Sci. Technol. 20 (3), 239–252.
Liu, B.Y.H., Agarwal, J.K., 1974. Experimental observation of aerosol deposition in turbulent flow. J. Aerosol Sci. 5, 145–155.
Maryon, R.H., Saltbones, J., Ryall, D.B., Bartnicki, J., Jakobsen, H.A., Berge, E., 1996. An intercomparison of three long range dispersion models developed for the UK meteorological office, DNMI and EMEP. UK Met Office Turbulence and Diffusion Note 234 ISBN: 82-7144-026-08.
Möller, U., Schumann, G., 1970. Mechanisms of transport from the atmosphere to the Earth's surface. Oceans and Atmospheres 75, 3013–3019.
Padro, J., 1996. Summary of ozone dry deposition velocity measurements and model estimates over vineyard, cotton, grass and deciduous forest in summer. Atmos. Environ. 30, 2363–2369.
Padro, J., Hartog, G., Neumann, H.H., 1991. An investigation of the ADOM dry deposition module using summertime O3 measurements above a deciduous forest. Atmos. Environ. 25, 1689–1704.
Paw, U.K.T., 1983. The rebound of particles from natural surfaces. J. Colloid Interface Sci. 93, 442–452.
Pellerin, G., Maro, D., Damay, P., Gehin, E., Connan, O., Laguionie, P., Hébert, D., Solier, L., Boulaud, D., Lamaud, E., Charrier, X., 2017. Aerosol particle dry deposition velocity above natural surfaces: quantification according to the particles diameter. J. Aerosol Sci. 114, 107–117.
Peters, K., Eiden, R., 1992. Modelling the dry deposition velocity of aerosol particles to a spruce forest. Atmos. Environ. 26A, 2555–2564.
Petroff, A., Mailliat, A., Amielh, M., Anselmet, F., 2008. Aerosol dry deposition on vegetative canopies. Part I: review of present knowledge. Atmos. Environ. 42, 3625–3653.
Pirrone, N., Keeler, G.J., Holsen, T.M., 1995. Dry deposition of trace elements to lake Michigan: a hybrid-receptor deposition modeling approach. Environ. Sci. Technol. 29 (8), 2112–2122.
Pryor, S.C., Barthelmie, R.J., Spaulding, A.M., Larsen, S.E., Petroff, A., 2009. Size-resolved fluxes of sub-100-nm particles over forests. J. Geophys. Res. 114 D18212.
Pryor, S.C., Gallagher, M., Sievering, H., Larsen, S.E., Barthelmie, R.J., Birsan, F., Nemitz, E., Rinne, J., Kulmala, M., Gro¨ Nholm, T., Taipale, R., Vesala, T., 2007. Review of measurement and modelling results of particle atmosphere–surface exchange 60 (1), 42–75.
Sehmel, G.A., 1973. Particle eddy diffusivities and deposition velocities for isothermal flow and smooth surfaces. J. Aerosol Sci. 4, 125–138.
Sehmel, G.A., 1980. Particle and gas dry deposition: a review. Atmos. Environ. 14, 983–1011.
Sehmel, G.A., Sutter, S.L., 1974. Particle deposition rates on a water surface as a function of particle diameter and air velocity. J. Rech. Atmos. 8, 912–920.
Seinfeld, J.H., Pandis, S.N., 1998. Atmospheric Chemistry and Physics. John Wiley&Sons, New York.
Slinn, S.A., Slinn, W.G.N., 1980. Predictions for particle deposition on natural waters. Atmos. Environ. 14, 1013–1016.
Slinn, W.G.N., 1982. Predictions for particle deposition to vegetative surfaces. Atmos. Environ. 16, 1785–1794.
Slinn, W.G.N., Hasse, L., Hicks, B.B., Hogan, A.W., Lal, D., Liss, P.S., Munnich, K.O., Sehmel, G.A., Vittorri, O., 1978. Some aspects of the transfer of atmospheric trace constituents past the air-sea interface. Atmos. Environ. 12, 2055–2087.
Tang, Y., Guo, B., Ranjan, D., 2015. Numerical simulation of aerosol deposition from turbulent flows using three-dimensional RANS and LES turbulence models. Engineering Applications of Computational Fluid Mechanics 9 (1), 174–186.
Venkatram, A., Pleim, J., 1999. The electrical analogy does not apply to modeling dry deposition of particles. Atmos. Environ. 33, 3075–3076.
Voldner, E.C., Barrie, L.A., Sirois, A., 1986. A literature review of dry deposition of oxides of sulphur and nitrogen with emphasis on long-range transport modelling in North America. Atmos. Environ. 20, 2101–2123.
Wesely, M.L., Cook, D.R., Hart, R.L., Speer, R.E., 1985. Measurements and parametrization of article sulfur deposition over grass. J. Geophys. Res. 90, 2131–2143.
Wesely, M.L., Doskey, P.V., Shannon, J., 2001. Deposition Parameterizations for the Industrial Source Complex (ISC3) Model, Report to U.S. EPA. Argonne National Laboratory, USA.
Wesely, M.L., Hicks, B.B., 1977. Some factors that affect the deposition rates of sulfur dioxide and similar gases to vegetation. J. Air Polka. Control Ass. 27, 1110–1116.
Zhang, J., Li, A., 2008. CFD simulation of particle deposition in a horizontal turbulent duct flow. Chem. Eng. Res. Des. 86, 95–106.
Zhang, J., Shao, Y., Huang, N., 2014. Measurements of dust deposition velocity in a wind-tunnel experiment. Atmos. Chem. Phys. 14, 8869–8882.
Zhang, L., Brook, J.R., Vet, R., 2003. A revised parameterization for gaseous dry deposition in air-quality models. Atmos. Chem. Phys. 3, 2067–2082.
Zhang, L., Gong, S., Padro, J., Barrie, L., 2001. A size-segregated particle dry deposition scheme for an atmospheric aerosol model. Atmos. Environ. 35, 549–560.
Zufall, M., Davidson, C., Caffrey, P., Ondov, J., 1998. Airborne concentration and dry deposition fluxes of particulate species to surrogate surfaces deployed in southern Lake Michigan. Environ. Sci. Technol. 32 (11), 1623–1628.

Abbreviations

C: pollutant concentration [g m^{-3}]
C_c: Cunningham slip correction factor [−]
D: particle's Brownian diffusivity [m^2 s^{-1}]
d_p: particle diameter [m]
F: pollutant flux [g m^{-2} s^{-1}]
g: gravity acceleration [m s^{-2}]
K: von Karman constant K = 0.4 [–]
K_B: Boltzmann constant, $K_B = 1.38\ 10^{-23}$ [J/K]
K_p: particle eddy diffusivity [m^2 s^{-1}]
L: Obhukov length [m]
m: non-dimensional number [−]
n: non-dimensional number [−]
QLS: Quasi-Laminar Sublayer [−]
r: total resistance [s m^{-1}]
r_a: aerodynamic resistance [s m^{-1}]
r_{db}: Brownian diffusion resistance [s m^{-1}]
r_{ii}: inertial impact resistance [s m^{-1}]
r_{ql}: quasi-laminar sublayer resistance [s m^{-1}]
r_{ti}: turbulent impact resistance [s m^{-1}]
Sc: Schmidt number [−]
SL: surface Layer [−]
St: Stokes number [−]
T: temperature [K]
U: horizontal mean flow velocity [m s^{-1}]
u_*: friction velocity [m s^{-1}]
v_d: deposition velocity [m s^{-1}]
v_s: settling velocity [m s^{-1}]
Z: quota to the ground reference level [m]
z_o: roughness length [m]
τ_+: non-dimensional particle relaxation time [−]
τ: particle relaxation time [s]
ρ_a: density of air [kg m^{-3}]
ρ_P: density of particle [kg m^{-3}]
μ_a: air dynamic viscosity $\mu_a = 1.82 \times 10^{-5}$ [kg m^{-1} s^{-1}]
ν_a: air kinematic viscosity $\nu_a = 1.51 \times 10^{-5}$ [m^2 s^{-1}]
λ_a: mean free path of air $\lambda_a = 0.067 \times 10^{-6}$ [m]